Communication

Direct Observation of Polymer-Stabilized Blue Phase I Structure with Confocal Laser Scanning Microscope

Kenji Higashiguchi, Kei Yasui, and Hirotsugu Kikuchi

J. Am. Chem. Soc., **2008**, 130 (20), 6326-6327 • DOI: 10.1021/ja801553g • Publication Date (Web): 26 April 2008

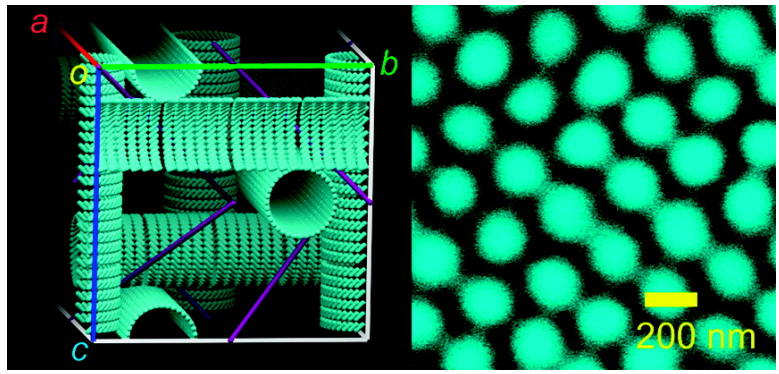

More About This Article

Additional resources and features associated with this article are available within the HTML version:

- Supporting Information
- Access to high resolution figures
- Links to articles and content related to this article
- Copyright permission to reproduce figures and/or text from this article

View the Full Text HTML

J|A|C|S
COMMUNICATIONS

Published on Web 04/26/2008

Direct Observation of Polymer-Stabilized Blue Phase I Structure with Confocal Laser Scanning Microscope

Kenji Higashiguchi,[†] Kei Yasui,[‡] and Hirotsugu Kikuchi*[,†]

Institute for Material Chemistry and Engineering, Kyushu University, Kasuga Park 6-1, Kasuga 816-8580, Japan, and Nissan Chemical Industries, Ltd., Tsuboi-cho 722-1, Funabashi, Chiba 274-8507, Japan

Received March 1, 2008; E-mail: kikuchi@cm.kyushu-u.ac.jp

Blue phases are exhibited by high chiral nematic liquid crystals and occur in a narrow temperature interval close to the clearing point. It is now generally accepted that the blue phases have a unique three-dimensional structure composed of double twist cylinders and disclinations,[1] and there are three blue phases, BP I, BP II, and BP III. As a result of intensive theoretical and experimental investigations, the structures of BP I and BP II are believed to be body centered cubic with space group symmetry $I4_132$ (O^8) (Figure 1) and simple cubic with $P4_232$(O^2), respectively.[2] Because of their three-dimensional structure with lattice periods of several hundred nanometers, the experimental methods based on Bragg diffractions, in a reciprocal space, in the range of visible light, such as selective reflection spectra and Kossel diagrams, have been key techniques to determine the structures.

Some experimental attempts to observe directly the real image of the blue phase structure by freeze-fracture electron microscopy with carbon replication technique and atomic force microscopy have been made, and periodic patterns resulting from BP I were actually observed.[3] However, the deformation of the lattice during sample preparations and the limitation of a temperature range appearing as blue phases make exact assignments of observed patterns difficult.

The authors have reported stabilization of blue phases over a temperature range more than 60 K.[4] These highly extended blue phases, so-called polymer-stabilized blue phases, were achieved through a photopolymerization of a small amount of monomer in the blue phase, creating a network structure of polymer chains probably along the disclination lines. The polymer-stabilized blue phases allow the direct observation of the structure in a wide temperature range including room temperature without lattice deformation.

Confocal laser scanning microscopy (CLSM) is a novel imaging technique that allows nondestructive optical observation with high resolution.[5] CLSM provides the image in a natural state, that is, the morphology can be observed without deformation because no fracture and no quenching of samples are required for obtaining an image.

Here we first show precise CLSM images with periodic patterns of the polymer-stabilized BP I without fracture and quenching and that each observed pattern was assigned to the lattice plane of the BP I structure model, bcc, proposed in general.

The samples of the polymer-stabilizing BP I for CLSM observations were prepared as follows: the mixture solution of the liquid crystal, the chiral dopant, monomers, and photoinitiator was sandwiched between a slide glass and a thin cover glass and left at the appropriate temperature until a desired blue phase texture appeared and was irradiated with UV light to polymerize the monomer (see Supporting Information).

The blue phases are characterized by their lattice constants of several hundred nanometers, derived from the Bragg reflections of circularly polarized light, which have been measured by reflection spectrometry

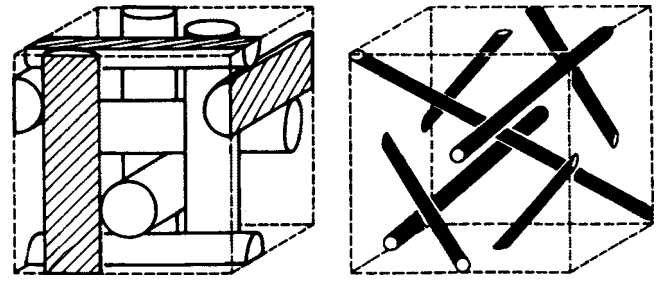

Figure 1. Schematic representation of a blue phase I. Arrangement of double twist cylinders (left) and the disclination lines (right). Figures from E. Dubois-Violette and B. Pansu.[6]

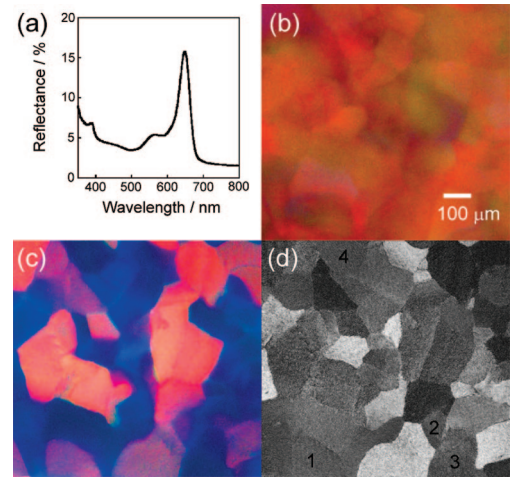

Figure 2. (a) The reflection spectrum of PSBP I; (b) the polarized transmission and (c) reflecting micrographs of the platelet texture; (d) low-magnification CLSM image for exactly the same region as (b) and (c).

and observed by a polarizing optical microscope. The reflection spectrum of the polymer-stabilized BP I used in this study is shown in Figure 2a. The polarized transmission and reflecting micrographs are shown in panels b and c of Figure 2, respectively. Some of the lattice orientations of the sample can be identified from the reflection spectra and the color of the photographs. In this case, the longest Bragg reflection, $\lambda_{max} = 650$ nm, was assigned to selective reflection from the {110} plane of the bcc lattice. Therefore, the red platelets in Figure 2c correspond to the domain orienting its [110] axis to the substrate surface normal. The bluish platelets should correspond to {200} or {211}. However, {200} and {211} were not distinguishable by polarizing optical microscopy though it was expected to show blue and black, respectively. The {111} does not show the Bragg diffraction because of the extinction rule of bcc symmetry. The light scattering which is increased with decreasing wavelength occurs in actual samples, as shown in Figure 2a. Therefore, every domain includes

[†] Kyushu University.
[‡] Nissan Chemical Industries, Ltd.

10.1021/ja801553g CCC: $40.75

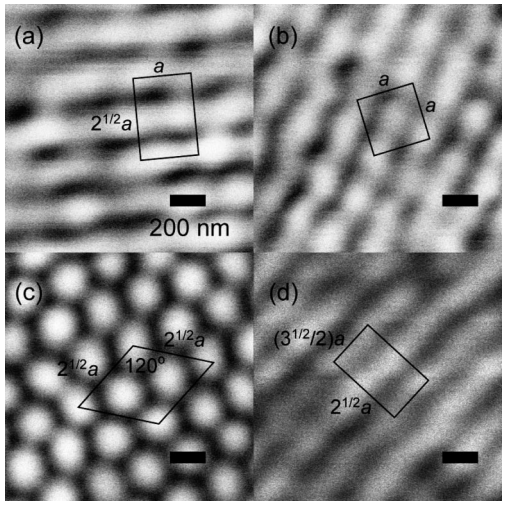

Figure 3. The magnificated images at the regions 1, 2, 3, and 4 in Figure 2d and geometrically expected 2D primitive cells. Here, the cubic lattice size a was determined from {111} to be 326.5 nm. (a) The image observed at the region 1 and a rectangle cell with $\boldsymbol{t}_1 = a$ and $\boldsymbol{t}_2 = 2^{1/2}a$ corresponding to {110}. (b) The image observed at the region 2 and a square cell with $\boldsymbol{t}_1 = \boldsymbol{t}_2 = a$ corresponding to {100}. (c) The image observed at the region 3 and a rhombus cell $\boldsymbol{t}_1 = \boldsymbol{t}_2 = 2^{1/2}a$ and $\gamma = 120°$ corresponding to {111}. (d) The image observed at the region 4 and a rectangle cell with $\boldsymbol{t}_1 = (3^{1/2}/2)a$, $\boldsymbol{t}_2 = 2^{1/2}a$ corresponding to {211}.

the bluish color arising from the light scattering on the base, then the domains of {100}, {111}, and {211} give very similar bluish color.

Figure 2d shows a CLSM observation photograph for exactly the same region as Figure 2c. A He−Ne laser with 543 nm was used as illumination light, which did not coincide with the wavelength of the Bragg diffractions of the sample. Most platelets showed a strong reflection signal at each appropriate focusing depth but did not focus at the same depth position between different platelets. The well-defined periodic patterns on the order of a couple hundred nanometers were observed in the bright platelets. The pattern was uniform within each platelet and discontinuously broken at grain boundaries. Several kinds of symmetry were found in the patterns depending on the platelet. The magnified images at the regions 1, 2, 3, and 4 in Figure 2d are shown in Figure 3a, b, c, and d, respectively. The observed 2D geometry of periodic structures in Figure 3a, b, c, and d can be explained by the cross-sectional morphologies of {110}, {100}, {111}, and {211}, respectively. At the cross sections of each plane in bcc with a lattice constant a, the lattice planes of a rectangle with $\boldsymbol{t}_1 = a$ and $\boldsymbol{t}_2 = 2^{1/2}a$, a square with $\boldsymbol{t}_1 = \boldsymbol{t}_2 = a$, a rhombus $\boldsymbol{t}_1 = \boldsymbol{t}_2 = 2^{1/2}a$ and $\gamma = 120°$, and a rectangle with $\boldsymbol{t}_1 = (3^{1/2}/2)a$, $\boldsymbol{t}_2 = 2^{1/2}a$ for {110}, {100}, {111}, and {211}, respectively, are expected to appear,[7] where $\boldsymbol{t}_1$ and $\boldsymbol{t}_2$ are the spacings of basic vectors of the 2D primitive cell and γ is the angle between them. The corresponding cells are drawn in Figure 3 when $a = 326.5$ nm, which was evaluated from the wavelength of selective reflection from {110}. Clearly the observed patterns can fit with the expected cells. From the account of the color of platelets, the assignment of planes mentioned above is reasonable because the domains having the pattern as Figure 3a exhibited a red reflection corresponding to the selective reflection at $\lambda_{max} = 650$ nm, and the other domains showed blue or dark blue. Thus we successfully observed the lattice structures of BP I directly.

In CLSM, a fluorescent emission in the sample is generally combined to obtain good contrast and high resolution. However, the pattern images as shown in Figure 3 were observed without a fluorescent specimen. The origin of the CLSM contrast giving the pattern for the blue phase should be cleared up for understanding more detailed structure from the observed images. A mirror reflection from the interface between the cover glass and the sample might give a patterned image depending on the spatial distribution of refractive index of the sample. Because the liquid crystal has anisotropy in the refractive index, the variation in molecular orientation at the interface should reflect the CLSM image. If the image originates in the mirror reflection at the interface, the image should be determined by the single depth focal point. However, we observed in-plane shift of the pattern depending on the in-focus depth (see Supporting Information), indicating clearly that the image does not result from the mirror reflection at the interface but from internal reflection in the sample. In general, the liquid crystals exhibit strong light scattering due to the director fluctuations as de Gennes formulated.[8] Therefore, the light back scattering depending on the molecular orientation in the bulk is a possible mechanism[9] of the well-ordered pattern reflecting the inner structure of BP I.

In conclusion, we observed directly the structure of polymer-stabilized BP I by CLSM. At least four types of periodic pattern images, attributable to {110}, {100}, {111}, and {211} planes of a bcc lattice in BP I, were found. The observed images are free from lattice deformation due to pretreatment of samples which has been a serious problem in other conventional methods.

Acknowledgment. This work was supported by Nissan Chemical Industries, Ltd.. We thank Chisso Co. Ltd. for providing the nematic mixture, JC-1041XX.

Supporting Information Available: Experimental procedures and *Z*-scanning image. This material is available free of charge via the Internet at http://pubs.acs.org.

References

(1) (a) Meiboom, S.; Sammon, M.; Barreman, D. W. *Phys. Rev. A* **1983**, *28*, 3553. (b) Wright, D. C.; Mermin, N. D. *Rev. Mod. Phys.* **1989**, *61*, 385–432.
(2) (a) Collings, P. J. *Nature's Delicate Phase of Matter*; Adam Hilger IOP Publishing Ltd: Bristol, U.K., 1990; p 196. (b) Crooker, P. P. *Chirality in Liquid Crystals*; Kitzerow, H. S., Bahr, C., Eds.; Springer-Verlag: New York, 2001.
(3) (a) Costello, M. J.; Meiboom, S.; Sammon, M. *Phys. Rev. A* **1984**, *29*, 2957–2959. (b) Delacroix, H.; Gilli, J. M.; Erk, I.; Mariani, P. *Phys. Rev. Lett.* **1992**, *69*, 2935–2938. (c) Gilli, J. M.; Kamaye, M.; Sixou, P. *Mol. Cryst. Liq. Cryst.* **1991**, *199*, 79–86. (d) Berreman, D. W.; Meiboom, S.; Zasadzinski, J. A.; Sammon, M. J. *Phys. Rev. Lett.* **1986**, *57*, 1737–1740. (e) Dumoulin, H.; Pieranski, P.; Delacroix, H.; Erk, I.; Gilli, J. M.; Lansac, Y. *Mol. Cryst. Liq. Cryst.* **1995**, *262*, 221–233. (f) Hauser, A.; Thieme, M.; Saupe, A.; Heppke, G.; Krüerke, D. J. *Mater. Chem.* **1997**, *7*, 2223–2229.
(4) Kikuchi, H.; Yokota, M.; Hisakado, Y.; Yang, H.; Kajiyama, T. *Nat. Mater.* **2002**, *1*, 64–68.
(5) Nakamura, O.; Kawata, S. *J. Opt. Soc. Am. A* **1990**, *7*, 522–526. (b) Streibl, N. *J. Opt. Soc. Am. A* **1985**, *2*, 121–127.
(6) Dubois-Violette, E.; Pansu, B. *Mol. Cryst. Liq. Cryst.* **1988**, *165*, 151–182.
(7) (a) Sigaud, G. *Mol. Cryst. Liq. Cryst. Lett. Sect.* **1978**, *41*, 129–135. (b) Barbet-Massin, R.; Cladis, P.; Pieranski, P. *Phys. Rev. A* **1984**, *30*, 1161–1164. (c) Stegemeyer, H.; Blumel, Th.; Hiltrop, K.; Onusseit, H.; Porsch, F. *Liq. Cryst.* **1986**, *1*, 3–28. (d) Blumel, Th.; Stegemeyer, H. *J. Cryst. Growth* **1984**, *66*, 163–168. (e) Pieranski, P.; Barbet-Massin, R.; Cladis, P. E. *Phys. Rev. A* **1985**, *31*, 3912–3923.
(8) (a) de Gennes, P. G.; Prost, J. *The Physics of Liquid Crystals*, 2nd ed.; Oxford: London, 1993. (b) de Gennes, P. G. *Mol. Cryst. Liq. Cryst.* **1969**, 325.
(9) (a) Akiyama, R.; Saito, Y.; Fukuda, A.; Kuze, E.; Goto, N. *Jpn. J. Appl. Phys.* **1980**, *19*, 1937–1945. (b) Akiyama, R.; Hasegawa, M.; Fukuda, A.; Kuze, E. *Jpn. J. Appl. Phys.* **1981**, *20*, 2019–2023.

JA801553G